Chapter 21

Extinction of Counterflow Premixed Laminar Flames

M. D. Smooke[1] and V. Giovangigli[2]

[1]Department of Mechanical Engineering, Yale University, New Haven, CT 06520
[2]Laboratoire de Mécanique Théorique, Université Paris VI, 4 Place Jussieu, 75230 Paris Cedex 05, France and Laboratoire d'Energétique, Ecole Centrale des Arts et Manufactures, 92290 Chatenay-Malabry, France

Problems in combustion and heat and mass transfer often depend upon one or more physical/chemical parameters. In many cases the combustion scientist is interested in knowing how the solution will behave if one or more of these parameters is varied. For some parameter regimes the governing equations can produce multiple solutions and the branches of the solution curve are linked via singular points. It is at these singular points, however, that the system exhibits special behavior. To be able to predict the solution structure in the neighborhood of these points, we employ a phase-space, pseudo arclength, continuation method that utilizes Newton-like iterations and adaptive gridding techniques. We apply the method in the solution of counterflow premixed laminar flames.

The modeling of steady-state problems in combustion and heat and mass transfer can often be reduced to the solution of a system of ordinary or partial differential equations. In many of these systems the governing equations are highly nonlinear and one must employ numerical methods to obtain approximate solutions. The solutions of these problems can also depend upon one or more physical/chemical parameters. For example, the parameters may include the strain rate or the equivalence ratio in a counterflow premixed laminar flame (1-2). In some cases the combustion scientist is interested in knowing how the system *will* behave if one or more of these parameters is varied. This information can be obtained by applying a first-order sensitivity analysis to the physical system (3). In other cases, the researcher may want to know how the system *actually* behaves as the parameters are adjusted. As an example, in the counterflow premixed laminar flame problem, a solution could be obtained for a specified value of the strain

0097-6156/87/0353-0404$06.00/0

rate; this solution could then be used as a starting estimate for a predictor-corrector continuation process in the same parameter. In many applications this procedure works well. However, when there are multiple solutions and the solution curve, when plotted versus the parameter that is varied, turns back on itself by passing through a singular point, this procedure encounters difficulty. It is at these singular points, however, that the system often experiences special behavior. For example, in the solution of counterflow premixed laminar flames, as the strain rate is increased past a critical value, the flame will extinguish. Similarly, for a given strain rate, as the equivalence ratio is either increased or decreased past a critical value, the flame will also extinguish. Hence, accurate knowledge of these points provides information about the flame's flammability limits.

To solve problems of physical interest numerically one often discretizes the spatial operators of the governing ordinary or partial differential equations with the result that the solution of the original continuous problem is reduced to finding an approximation to this solution at each point of a discrete mesh. The discrete nonlinear equations can be solved by Newton's method, or a variant thereof. In addition, if the solution contains regions of high spatial activity, then it is essential for reasons of both efficiency and accuracy that adaptive spatial grids be employed. However, in the neighborhood of singular points, i.e., turning points, where the derivative of the solution curve with respect to the parameter possesses a vertical tangent, Newton's method encounters difficulties. To be able to follow the solution in the neighborhood of turning points, we modify the basic solution algorithm and employ a path tracing continuation method in which points on the arc of solutions are computed. In this paper we apply a powerfull combination of continuation techniques, Newton-like iterations and adaptive gridding in the study of the extinction of strained premixed laminar flames. In particular, we investigate the extinction of hydrogen-air flames by a combination of strain rate and equivalence ratio variation. The governing conservation equations are modeled with complex transport and detailed chemical kinetics.

Problem Formulation

Strained premixed laminar flames have played an important role in recent theories of turbulent premixed combustion. The reacting surface in such models can be viewed as being composed of a number of laminar flamelets (see e.g., Libby and Bray, (4), Libby and Williams, (5) and Bray, Libby and Moss, (6). The flamelets are often modeled by considering counterflowing streams of reactants or counterflowing streams of reactants and products. From an experimental viewpoint, these flames can be produced when a single reactant stream impinges on an adiabatic wall or when two counterflowing reactant streams (or a reactant stream and a product stream) emerge from two counterflowing coaxial jets. In the neighborhood of the stagnation point produced by these flows, a chemically reacting boundary layer is established. The governing conservation

equations can be reduced to a set of nonlinear two-point boundary value problems along the stagnation point streamline. When there is a single reactant jet, only one reaction zone is produced. However, if there are two reactant streams and each has the same exit velocity and equivalence ratio, then a double flame is produced with a plane of symmetry through the stagnation point and parallel to the two jets (see Figure 1).

In this paper we consider doubly premixed laminar flames produced by two counterflowing coaxial jets. By applying appropriate boundary conditions at the plane of symmetry, the model we consider is, in principle, equivalent to that of a single reactant stream impinging on an adiabatic wall with slip. Our model for counterflowing premixed laminar flames assumes a laminar, stagnation point flow. We model the system by employing a boundary layer approximation. The governing equations for mass, momentum, chemical species and energy in rectangular coordinates can be written in the form (2)

$$\frac{\partial(\rho u)}{\partial x} + \frac{\partial(\rho v)}{\partial y} = 0 \tag{2.1}$$

$$\rho u\frac{\partial u}{\partial x} + \rho v\frac{\partial u}{\partial y} + \frac{\partial p}{\partial x} - \frac{\partial}{\partial y}\left(\mu\frac{\partial u}{\partial y}\right) = 0 \tag{2.2}$$

$$\rho u\frac{\partial Y_k}{\partial x} + \rho v\frac{\partial Y_k}{\partial y} + \frac{\partial}{\partial y}\left(\rho Y_k V_{ky}\right) - \dot{w}_k W_k = 0, \quad k = 1, 2, \ldots, K \tag{2.3}$$

$$\rho u c_p\frac{\partial T}{\partial x} + \rho v c_p\frac{\partial T}{\partial y} - \frac{\partial}{\partial y}\left(\lambda\frac{\partial T}{\partial y}\right) + \sum_{k=1}^{K}\rho Y_k V_{ky} c_{pk}\frac{\partial T}{\partial y} + \sum_{k=1}^{K}\dot{w}_k W_k h_k = 0 \tag{2.4}$$

The system is closed with the ideal gas law,

$$\rho = \frac{p\overline{W}}{RT} \tag{2.5}$$

In these equations x and y denote independent spatial coordinates; T, the temperature; Y_k, the mass fraction of the k^{th} species; p, the pressure; u and v the tangential and the transverse components of the velocity, respectively; ρ, the mass density; W_k, the molecular weight of the k^{th} species; $\overline{W}$, the mean molecular weight of the mixture; R, the universal gas constant; λ, the thermal conductivity of the mixture; c_p, the constant pressure heat capacity of the mixture; c_{p_k}, the constant pressure heat capacity of the k^{th} species; $\dot{w}_k$, the molar rate of production of the k^{th} species per unit volume; h_k, the specific enthalpy of the k^{th} species; μ the viscosity of the mixture and V_{ky}, the diffusion velocity of the k^{th} species in the y direction. The free stream tangential and transverse velocities at the edge of the boundary layer are given by $u_e = ax$ and $v_e = -ay$, respectively, where a is the strain rate. The strain rate is a measure of the "stretch" in the flame due to the imposed flow. The form of the chemical production rates and the diffusion velocities can be found in (7-8).

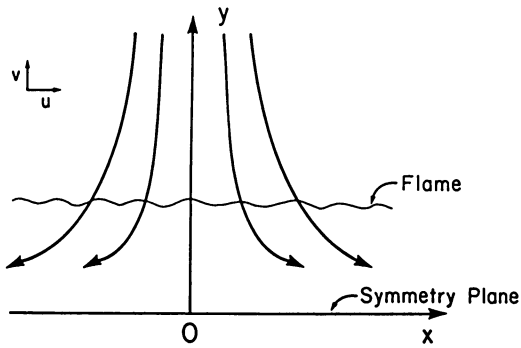

Figure 1. Schematic of the stagnation point flow configuration.

Upon introducing the notation

$$f' = \frac{u}{ax} \tag{2.6}$$

$$V = \rho v \tag{2.7}$$

where f' is related to the derivative of a modified stream function (see e.g., Dixon-Lewis et al., (9)), the boundary layer equations can be transformed into a system of ordinary differential equations valid along the stagnation-point streamline $x = 0$. For a system in rectangular coordinates, we have

$$\frac{dV}{dy} + a\rho f' = 0 \tag{2.8}$$

$$\frac{d}{dy}\left(\mu\frac{df'}{dy}\right) - V\frac{df'}{dy} + a(\rho_e(\phi) - \rho(f')^2) = 0 \tag{2.9}$$

$$-\frac{d}{dy}(\rho Y_k V_{k_y}) - V\frac{dY_k}{dy} + \dot{w}_k W_k = 0, \quad k = 1, 2, \ldots, K \tag{2.10}$$

$$\frac{d}{dy}\left(\lambda\frac{dT}{dy}\right) - c_p V\frac{dT}{dy} - \sum_{k=1}^{K}\rho Y_k V_{k_y} c_{pk}\frac{dT}{dy} - \sum_{k=1}^{K}\dot{w}_k W_k h_k = 0 \tag{2.11}$$

where ρ_e refers to the density at the edge of the boundary layer. The system is again closed with the ideal gas law.

Complete specification of the problem requires that boundary conditions be imposed at each end of the computational domain. At $y = 0$ we have

$$V = 0 \tag{2.12}$$

$$\frac{df'}{dy} = 0 \tag{2.13}$$

$$\frac{dY_k}{dy} = 0, \quad k = 1, 2, \ldots, K \tag{2.14}$$

$$\frac{dT}{dy} = 0 \tag{2.15}$$

and as $y \to \infty$

$$f' = 1 \tag{2.16}$$

$$Y_k = Y_{k_e}(\phi), \quad k = 1, 2, \ldots, K \tag{2.17}$$

$$T = T_e \tag{2.18}$$

where the temperature T_e and mass fractions $Y_{k_e}(\phi), k = 1, 2, \ldots, K$ at the edge of the boundary layer are specified.

We observe that, in addition to the strain rate a, the computational model depends on the equivalence ratio ϕ which is a measure of the relative proportion

of fuel to air in the reactant stream. If the strain rate is increased past a critical value the flame will extinguish. Similarly, if the equivalence ratio is either increased or decreased past a critical point, the flame will extinguish. Hence, accurate knowledge of the behavior of counterflow premixed flames as these quantities are varied can provide information about the flame's flammability limits. Our goal is to predict accurately and efficiently these extinction limits. This information can then be used in theories of turbulent premixed combustion.

Method of Solution

Solution of the equations in (2.8-2.18) proceeds with an adaptive nonlinear boundary value method. The solution procedure has been discussed in detail elsewhere (10) and we outline only the essential features here. Our goal is to obtain a discrete solution of the governing equations on the mesh $\mathcal{M}$

$$\mathcal{M} = \{0 = y_0 < y_1 < \ldots < y_m = L\} \tag{3.1}$$

where $h_j = y_j - y_{j-1}, j = 1, 2, \ldots, m$, and where the value of L is related to the jet separation distance.

With the continuous differential operators replaced by difference expressions, we convert the problem of finding an analytic solution of the governing equations to one of finding an approximation to this solution at each point of the mesh $\mathcal{M}$. We seek the solution U^* of the nonlinear system of difference equations

$$F(U) = 0 \tag{3.2}$$

For an initial solution estimate U^0 that is sufficiently "close" to U^*, the system of equations in (3.2) can be solved by Newton's method. We write

$$J(U^k)\left(U^{k+1} - U^k\right) = -\lambda_k F(U^k), \quad k = 0, 1, \ldots \tag{3.3}$$

where U^k denotes the k^{th} solution iterate, λ_k the k^{th} damping parameter $(0 < \lambda \leq 1)$ which should be chosen to ensure a reduction in the size of the Newton corrections at each iteration (see, e.g., Deuflhard, (11)) and $J(U^k) = \partial F(U^k)/\partial U$ the Jacobian matrix. A system of linear block tridiagonal equations must be solved at each iteration for corrections to the previous solution vector. In practice, a modified Newton method is employed in which the Jacobian is re-evaluated periodically (12).

Once a solution is obtained on an initial mesh, we adapt the grid in regions where the dependent solution components exhibit high spatial activity. We determine the mesh by subequidistributing the difference in the components of the discrete solution and its gradient between adjacent mesh points (10). Upon denoting the vector of N dependent solution components by $\tilde{U} = [\tilde{U}_1, \tilde{U}_2, \ldots, \tilde{U}_N]^T$, we seek a mesh $\mathcal{M}$ such that

$$\int_{y_j}^{y_{j+1}} \left|\frac{d\tilde{U}_i}{dy}\right| \, dy \quad \leq \quad \delta \left| \max_{0 \leq y \leq L} \tilde{U}_i - \min_{0 \leq y \leq L} \tilde{U}_i \right| \qquad \begin{matrix} j = 0, 1, \ldots, m-1 \\ i = 1, 2, \ldots, N \end{matrix} \tag{3.4}$$

and

$$\int_{y_j}^{y_{j+1}} \left|\frac{d^2\tilde{U}_i}{dy^2}\right| \, dy \leq \gamma \left| \max_{0\leq y\leq L} \frac{d\tilde{U}_i}{dy} - \min_{0\leq y\leq L} \frac{d\tilde{U}_i}{dy} \right| \qquad \begin{matrix} j = 1,2,\ldots,m-1 \\ i = 1,2,\ldots,N \end{matrix} \tag{3.5}$$

where δ and γ are small numbers less than one and the maximum and minimum values of $\tilde{U}_i$ and $d\tilde{U}_i/dy$ are obtained from a converged numerical solution on a previously determined mesh. We also impose the added constraint that the mesh produced by employing (3.4) and (3.5) be locally bounded. This smooths out rapid changes in the size of the mesh intervals. The advantage of this gridding procedure is that most of the expensive Jacobian evaluations are performed on relatively coarse grids and once the grid is sufficiently refined, Newton's method usually converges with only one or two iterations. The method also takes into account every component of the solution in forming a new mesh.

Arclength Continuation

Procedures enabling the calculation of bifurcation and limit points for systems of nonlinear equations have been discussed, for example, by Keller (13) Heinemann et al. (14-15) and Chan (16). In particular, in the work of Heineman et al., a version of Keller's pseudo-arclength continuation method was used to calculate the multiple steady-states of a model one-step, nonadiabatic, premixed laminar flame (Heinemann et al., (14)) and a premixed, nonadiabatic, hydrogen-air system (Heinemann et al., (15)).

In our computational model the strain rate and the equivalence ratio are the natural bifurcation parameters. If we denote either of these parameters by α, then the system of equations in (3.2) can be written in the form

$$F(U,\alpha) = 0 \tag{4.1}$$

where specific reference to the parametric dependence of F on α has been made. As the flame nears extinction (either from an increase in the strain rate or from a change in the equivalence ratio), the maximum value of the temperature decreases. At the extinction point the Jacobian of the system is singular. To alleviate the computational difficulties, a modified form of the governing equations is solved (13). We introduce the parameter α as a new dependent variable. The vector of dependent variables $(U,\alpha)^T$ can now be considered functions of a new independent parameter s. If we define

$$Z(s) = (U(s),\alpha(s))^T \tag{4.2}$$

then the new problem we want to solve is given by

$$G(Z,s) = 0 \tag{4.3}$$

where

$$G(Z,s) = \begin{bmatrix} F(U(s),\alpha(s)) \\ N(U(s),\alpha(s),s) \end{bmatrix} = \begin{bmatrix} F(Z(s)) \\ N(Z(s),s) \end{bmatrix} \tag{4.4}$$

and where N is an arbitrary normalization. The normalization is chosen such that s approximates the arclength of the solution branch in the space (U, α).

The Jacobian of the new system can be written in the form

$$J(Z,s) = G_Z(Z,s) = \begin{bmatrix} F_U(U(s),\alpha(s)) & F_\alpha(U(s),\alpha(s)) \\ N_U(U(s),\alpha(s),s) & N_\alpha(U(s),\alpha(s),s) \end{bmatrix} \tag{4.5}$$

where F_U, F_α, N_U and N_α denote the appropriate partial derivatives. It can be shown that at a simple turning point, even though F_U is singular J is not. We point out that the Jacobian of the system in (3.2) is block tridiagonal. However, after introduction of α as a dependent variable along with the extra normalization condition, the block tridiagonal structure of the Jacobian is destroyed. For the normalizations considered by Heinemann et al. (14-15) (see also Keller, (13)) this is the case. Although solution of the system of linear equations corresponding to (4.3) can proceed by methods discussed in (16), we would like to maintain the basic block tridiagonal structure of the Jacobian. In this way we can utilize the solution method used in solving adiabatic, premixed, laminar flames (17), burner-stabilized, premixed, laminar flames (10), counterflow, laminar, diffusion flames (18), and the extinction problems we consider here (2).

For each value of the parameter s, we want to obtain the corresponding value of α and the remaining dependent solution components. We point out that, for each value of the pseudo-arclength, α is constant. It satisfies the trivial differential equation

$$\frac{d}{dy}(\alpha) = 0 \tag{4.6}$$

Hence, we can maintain the block tridiagonal structure of the Jacobian in (4.5) if we introduce the parameter α as a dependent variable at m of the $m+1$ grid points and if we specify a normalization condition at the remaining grid point that does not introduce nonzero Jacobian entries outside of the three block diagonals. The success of this procedure depends upon the choice of the normalization condition.

In flame extinction studies the maximum temperature is used often as the ordinate in bifurcation curves. In the counterflowing premixed flames we consider here, the maximum temperature is attained at the symmetry plane $y = 0$. Hence, it is natural to introduce the temperature at the first grid point along with the reciprocal of the strain rate or the equivalence ratio as the dependent variables in the normalization condition. In this way the block tridiagonal structure of the Jacobian can be maintained. The final form of the governing equations we solve is given by (2.8)-(2.18), (4.6) and the normalization condition

$$N = \frac{dT(0,s_0)}{ds}(T(0,s)-T(0,s_0)) + \frac{d}{ds}(\alpha(0,s_0))\,(\alpha(0,s)-\alpha(0,s_0)) - (s-s_0) = 0 \tag{4.7}$$

where α represents either $1/a$ or ϕ. This normalization is such that s approximates the arclength of the solution branch in the space $(T(0), \alpha)$.

In Supercomputer Research in Chemistry and Chemical Engineering; Jensen, Klavs F., et al.;
ACS Symposium Series; American Chemical Society: Washington, DC, 1987.

Numerical Results

In this section we apply the adaptive boundary value solution procedure and the pseudo-arclength continuation method to a set of strained premixed hydrogen-air flames. Our goal is to predict accurately and efficiently the extinction behavior of these flames as a function of the strain rate and the equivalence ratio. Detailed transport and complex chemical kinetics are included in all of the calculations. The reaction mechanism for the hydrogen-air system is listed in Table I (17).

Strain Rate Extinction. We performed a sequence of strain rate calculations for an 8.4% and a 9.3% (mole fraction) hydrogen-air flame. The equivalence ratios of these flames are $\phi = 0.219$ and $\phi = 0.245$, respectively. In both cases the Lewis number of the deficient reactant (hydrogen) was significantly less than one. In particular, at the input jet, the Lewis numbers were equal to 0.29 for both the 8.4% flame and the 9.3% flame. We also found that these values did not change by more than 15% through the flame.

A number of theoretical (5), (19-23), experimental (24-28) and computational (2), (23), (29-32), studies of premixed flames in a stagnation point flow have appeared recently in the literature. In many of these papers it was found that the Lewis number of the deficient reactant played an important role in the behavior of the flames near extinction. In particular, in the absence of downstream heat loss, it was shown that extinction of strained premixed laminar flames can be accomplished via one of the following two mechanisms. If the Lewis number (the ratio of the thermal diffusivity to the mass diffusivity) of the deficient reactant is greater than a critical value, $Le_c > 1$, then extinction can be achieved by flame stretch alone. In such flames (e.g., rich methane-air and lean propane-air flames) extinction occurs at a finite distance from the plane of symmetry. However, if the Lewis number of the deficient reactant is less than this value (e.g., lean hydrogen-air and lean methane-air flames), then extinction occurs from a combination of flame stretch and incomplete chemical reaction. Based upon these results we anticipate that the Lewis number of hydrogen will play an important role in the extinction process.

For an initial value of the strain rate, the adaptive boundary value method was used to obtain a solution on a computational domain of one cm. In Figures 2 and 3 we plot the temperature and the normal velocity component as a function of the distance from the symmetry plane for the 9.3% (mole fraction) flame with a strain rate of $a = 200\ \text{sec}^{-1}$. In Figures 4 and 5 we illustrate the major and minor species profiles. As we found in the solution of freely propagating premixed hydrogen-air flames, the HO_2 and H_2O_2 profiles peak before the flame zone. The remaining radical species peak in the region of maximum temperature. Once the initial strain rate calculation was completed, the modified arclength continuation procedure was implemented to obtain profiles of the maximum temperature versus the inverse of the strain rate. For each hydrogen-air mixture, the equidistribution procedure discussed in (3.4)-(3.5) was used to determine the mesh for the continuation steps. Each solution contained between

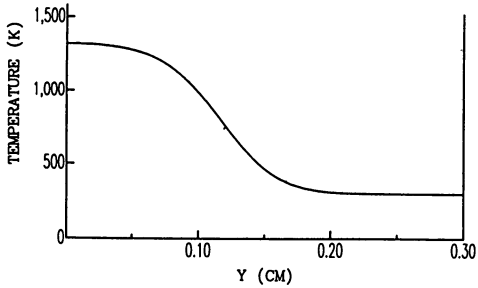

Figure 2. Temperature profile in K for the 9.3% (mole fraction) hydrogen-air flame with a strain rate of $a = 200$ sec^{-1}.

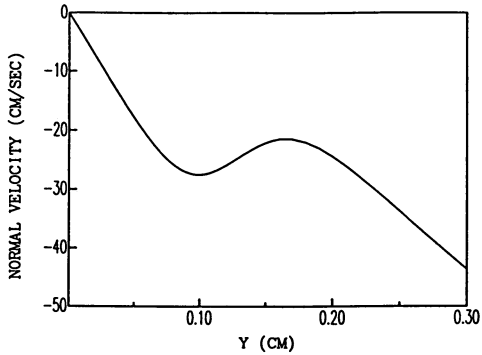

Figure 3. Normal velocity profile in cm/sec for the 9.3% (mole fraction) hydrogen air flame with a strain rate of $a = 200$ sec^{-1}.

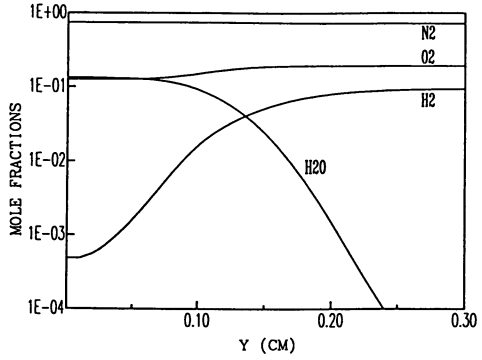

Figure 4. Major species profiles for the 9.3% (mole fraction) hydrogen-air flame with a strain rate of $a = 200$ sec^{-1}.

TABLE I

Hydrogen-Air Reaction Mechanism
Rate Coefficients In The Form $k_f = AT^{\beta}\exp(-E_0/RT)$.
Units are moles, cubic centimeters, seconds, Kelvins and calories/mole

	REACTION	A	β	E
1.	$H_2 + O_2 \rightleftharpoons 2OH$	1.70E+13	0.000	47780.
2.	$OH + H_2 \rightleftharpoons H_2O + H$	1.17E+09	1.300	3626.
3.	$H + O_2 \rightleftharpoons OH + O$	5.13E+16	-0.816	16507.
4.	$O + H_2 \rightleftharpoons OH + H$	1.80E+10	1.000	8826.
5.	$H + O_2 + M \rightleftharpoons HO_2 + M^a$	2.10E+18	-1.000	0.
6.	$H + O_2 + O_2 \rightleftharpoons HO_2 + O_2$	6.70E+19	-1.420	0.
7.	$H + O_2 + N_2 \rightleftharpoons HO_2 + N_2$	6.70E+19	-1.420	0.
8.	$OH + HO_2 \rightleftharpoons H_2O + O_2$	5.00E+13	0.000	1000.
9.	$H + HO_2 \rightleftharpoons 2OH$	2.50E+14	0.000	1900.
10.	$O + HO_2 \rightleftharpoons O_2 + OH$	4.80E+13	0.000	1000.
11.	$2OH \rightleftharpoons O + H_2O$	6.00E+08	1.300	0.
12.	$H_2 + M \rightleftharpoons H + H + M^b$	2.23E+12	0.500	92600.
13.	$O_2 + M \rightleftharpoons O + O + M$	1.85E+11	0.500	95560.
14.	$H + OH + M \rightleftharpoons H_2O + M^c$	7.50E+23	-2.600	0.
15.	$H + HO_2 \rightleftharpoons H_2 + O_2$	2.50E+13	0.000	700.
16.	$HO_2 + HO_2 \rightleftharpoons H_2O_2 + O_2$	2.00E+12	0.000	0.
17.	$H_2O_2 + M \rightleftharpoons OH + OH + M$	1.30E+17	0.000	45500.
18.	$H_2O_2 + H \rightleftharpoons HO_2 + H_2$	1.60E+12	0.000	3800.
19.	$H_2O_2 + OH \rightleftharpoons H_2O + HO_2$	1.00E+13	0.000	1800.

[a] Third body efficiencies: $k_5(H_2O) = 21k_5(Ar)$, $k_5(H_2) = 3.3k_5(Ar)$, $k_5(N_2) = k_5(O_2) = 0$.

[b] Third body efficiencies: $k_{12}(H_2O) = 6k_{12}(Ar)$, $k_{12}(H) = 2k_{12}(Ar)$, $k_{12}(H_2) = 3k_{12}(Ar)$.

[c] Third body efficiency: $k_{14}(H_2O) = 20k_{14}(Ar)$.

50-70 adaptively chosen grid points. In addition, the Euler-Newton continuation procedure was used to help obtain solutions (physical and unphysical) for both increasing and decreasing values of the strain rate.

In Figure 6 we plot the maximum temperature versus the inverse of the strain rate for the 8.4% and 9.3% (mole fraction) hydrogen-air flames. Each C-shaped extinction curve was the result of 84-93 continuation steps. If we consider the 9.3% curve, we see that as we move along the upper branch in the direction of increasing strain rate, the peak temperature first increases and then decreases. Ultimately, as the value of $dT_{max}/d(1/a) \rightarrow \infty$, the flames extinguish ($a_{ext} = 1443$ sec $^{-1}$ for the 9.3 % flame and $a_{ext} = 760$ sec $^{-1}$ for the 8.3 % flame). We can, however, continue past the extinction point with the arclength procedure. We find that, as the strain rate begins to decrease, the peak temperature continues to fall. In the absence of Hopf bifurcation, the upper branch represents physical solutions and the lower branch unphysical solutions. The increase in the temperature can be attributed to the additional heat release

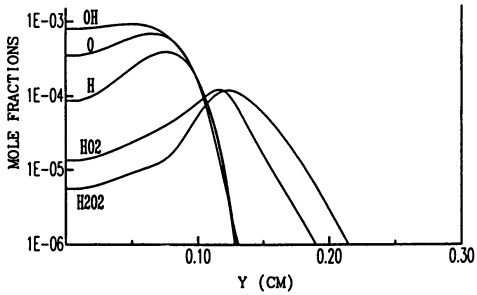

Figure 5. Minor species profiles for the 9.3% (mole fraction) hydrogen-air flame with a strain rate of $a = 200\ \text{sec}^{-1}$.

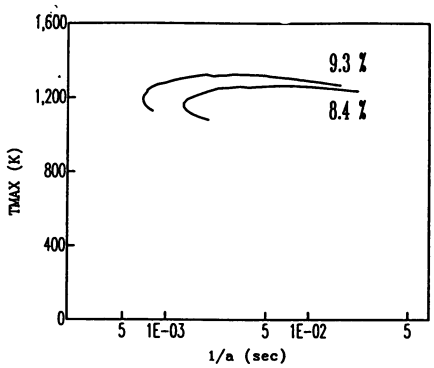

Figure 6. C-shaped extinction curves illustrating the maximum temperature versus the inverse of the strain rate for the 8.4% and 9.3% (mole fraction) hydrogen-air flames.

that results from the diffusion of hydrogen (the deficient reactant) from the unburnt mixture into the reaction zone. This excess heat release is larger than the conductive heat flow from the reaction zone to the unburnt mixture. As the strain rate continues to increase, however, the peak temperature finally decreases. Eventually, as the reaction zone is pressed against the stagnation surface, incomplete combustion occurs due to the decreased residence time and the flame extinguishes.

It is interesting to note that the adiabatic flame temperature of a freely propagating (unstrained) 9.3% (mole fraction) hydrogen-air flame is 1046 K while the peak temperature in Figure 6 is approximately 1324 K. Similarly, the adiabatic flame temperature of a freely propagating 8.4% (mole fraction) hydrogen-air flame is 977 K while the peak temperature in Figure 6 is 1264 K. Hence, we have Lewis number temperature increases of 278 K and 287 K, respectively. These peak temperatures as well as the extinction behavior illustrated in Figure 6 are in excellent qualitative agreement with the asymptotic results of Libby and Williams (22). Good quantitative agreement, however, is, in general, not feasible (Giovangigli and Candel, (23)).

If we continue the arclength process such that the strain rate decreases even further, we will continue to move along the unphysical branch and eventually reach another turning point–an ignition point. After the ignition point is passed, we will move on to the extinguished solution branch. We have not calculated the ignition points since they occur at strain rates so low that the corresponding flames are physically uninteresting and it is impossible to stabilize such a flame in the laboratory (see also Smith et al., (29)).

Lean and Rich Extinction. Extinction of strained premixed laminar flames can also be obtained (for a given strain rate) by adjusting the equivalence ratio. In particular, experimental results show that as the equivalence ratio is either increased or decreased past a critical point, the flame extinguishes. Starting with a hydrogen-air flame having an equivalence ratio $\phi = 0.245$ (9.3 % mole fraction) and a strain rate of $a = 1000\,\mathrm{sec}^{-1}$ which was obtained during the strain rate extinction calculations, the Euler-Newton adaptive continuation procedure was used to obtain solutions (physical and unphysical) for all values of the equivalence ratio. Each solution contained between 80-120 adaptively chosen grid points.

Starting from stoichiometric conditions ($\phi = 1$) and then proceeding in the lean direction ($\phi < 1$), we anticipate that the peak flame temperature will be reduced gradually. In addition, as the maximum temperature is lowered and the corresponding adiabatic flame speed of an unstrained ($a = 0$) flame is reduced, we anticipate that the flame will move closer to the plane of symmetry. Ultimately, as the fuel to air ratio is lowered below a critical value, radical production in the flame will be severely restricted and the flame will extinguish (lean extinction). The arclength continuation procedure will then generate unphysical solutions for additional continuation steps until a maximum value of the

equivalence ratio is reached. At this point (rich extinction) physical solutions will again be generated and the maximum flame temperature will begin to rise and the distance of the flame from the plane of symmetry will increase as well.

The adaptive continuation method was able to generate closed response curves illustrating these phenomena. In particular, in Figure 7 we illustrate the maximum temperature versus the equivalence ratio for a hydrogen-air system with $a = 1000$ sec^{-1}. We observe a 1500 K temperature variation among all the flames computed. The lean extinction occurred at $\phi = 0.227$ with $T = 1177$ K and the rich extinction at $\phi = 4.6$ with $T = 1256$ K. Variations in the peak temperature occur over a much smaller range of equivalence ratios for lean systems than under rich conditions. In Figure 8 we illustrate the distance of the flame from the plane of symmetry. The flame can shift its position by almost 0.9 cm from lean to slightly rich conditions and then back again to very rich conditions. In particular, the position of the flame from the symmetry plane was equal to 0.03556 cm at the lean extinction limit, 0.8639 cm at its furthest point and 0.1073 cm at the rich extinction limit. A total of 2500 continuation steps were used in generating the closed curves in Figures 7 and 8. In all cases the adaptive mesh was able to maintain resolution in the flame zone as the flame's position adjusted accordingly.

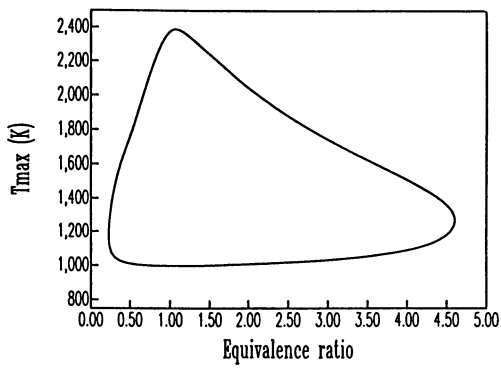

Figure 7. Extinction curve illustrating the maximum temperature versus the equivalence ratio for hydrogen-air flames with a strain rate of $a = 1000$ sec^{-1}.

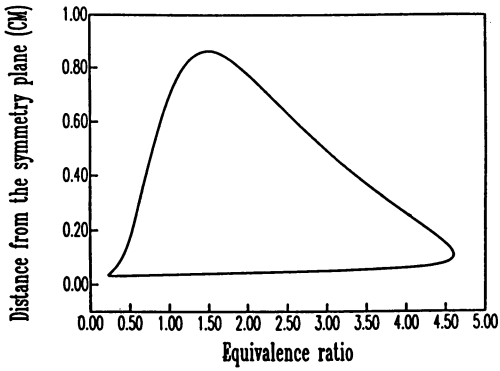

Figure 8. Distance of the flame from the symmetry plane versus the equivalence ratio for hydrogen-air flames with a strain rate of $a = 1000\ \text{sec}^{-1}$.

Acknowledgment

The research was supported in part by Direction des Recherches et Etudes Techniques and the Office of Naval Research. We would like to thank the Scientific Council of the Centre de Calcul Vectoriel pour la Recherche for providing access to a CRAY-1 computer and the Centre Inter Regional de Calcul Electronique for providing computational resources. In addition, we would like to thank Professors S. Candel and G. Duvaut for their support and helpful discussions.

References

1. Giovangigli, V. and Smooke, M. D. (1987). J. Comp. Phys. **68**, p. 327.
2. Giovangigli, V. and Smooke, M. D. (1987). Comb. Sci. and Tech. **53**, p. 23.
3. Smooke, M. D., Reuven, Y., Rabitz, H. and Dryer, F. L., to be published in Comb. Sci. and Tech., (1987).
4. Libby, P. A. and Bray, K. N. C (1980). *Comb. and Flame* **39**, p. 33.
5. Libby, P. A. and Williams, F. A. (1982). *Comb. and Flame* **44**, p. 287.
6. Bray, K. N. C., Libby, P. A. and Moss, J. B. (1984). *Comb. Sci. and Tech.* **41**, p. 143.
7. Kee, R. J., Miller, J. A. and Jefferson, T. H. (1980). Sandia National Laboratories Report, SAND80-8003.
8. Kee, R. J., Warnatz, J., and Miller, J. A. (1983). Sandia National Laboratories Report, SAND83-8209.
9. Dixon-Lewis, G., David, T., Haskell, P. H., Fukutani, S., Jinno, H., Miller, J. A., Kee, R. J., Smooke, M. D., Peters, N., Effelsberg, E., Warnatz, J. and Behrendt, F. (1982). Twentieth Symposium (International) on Combustion, Reinhold, New York, p. 1893.
10. Smooke, M. D. (1982). *J. Comp. Phys.* **48**, p. 72.
11. Deuflhard, P. (1974). *Numer. Math.* **22**, p. 289.

12. Smooke, M. D. (1983). *J. Opt. Theory and Appl.* **39**, p. 489.
13. Keller, H. B. (1977). in Applications of Bifurcation Theory, P. Rabinowitz, Ed., Academic Press, New York.
14. Heinemann, R. F., Overholser, K. A. and Reddien, G. W. (1979). *Chem Eng. Sci.* **34**, p. 833.
15. Heinemann, R. F., Overholser, K. A. and Reddien, G. W. (1980). *AIChE Journal* **26**, p. 725.
16. Chan, T. (1984). in Numerical Methods for Bifurcation Problems, T. Kupper, H. Mittelmann and H. Weber, Eds., Birkhauser Verlag, Basel.
17. Smooke, M. D., Miller, J. A. and Kee, R. J. (1983). *Comb. Sci. and Tech.* **34**, p. 79.
18. Smooke, M. D., Miller, J. A. and Kee, R. J. (1985). in Numerical Boundary Value ODEs, U. M. Ascher and R. D. Russell, Eds., Birkhauser, Basel.
19. Sivashinsky, G. I. (1976). *ACTA Astronautica* **3**, p. 889.
20. Buckmaster, J. (1982). Seventeenth Symposium (International) on Combustion, Reinhold, New York, p. 835.
21. Libby, P. A., Liñàn, A. and Williams, F. A. (1983). *Comb. Sci. and Tech.* **34**, p. 257.
22. Libby, P. A. and Williams, F. A. (1984). *Comb. Sci. and Tech.* **37**, p. 221.
23. Giovangigli, V. and Candel, S. (1986). *Comb. Sci. and Tech.*, in press.
24. Fang, M., Schmitz, R. A. and Ladd, R. G. (1971). *Comb. Sci. and Tech.* **4**, p. 143.
25. Law, C. K., Ishizuka , S. and Mizomoto, M. (1981). *Eighteenth Symposium (International) on Combustion*, Reinhold, New York, p. 1791.
26. Ishizuka, S. and Law C. K. (1982). *Nineteenth Symposium (International) on Combustion*, Reinhold, New York, p. 327.
27. Sato, J. (1982). *Nineteenth Symposium (International) on Combustion*, Reinhold, New York, p. 1541.
28. Tsuji, H. and Yamaoka, I. (1982). Nineteenth Symposium (International) on Combustion, Reinhold, New York, p. 1533.
29. Smith, H. W., Schmitz, R. A. and Ladd, R. G. (1971). *Comb. Sci. and Tech.* **4**, p. 131.
30. Sato, J. and Tsuji, H. (1978). in Proceedings of the Sixteenth Japanese Symposium on Combustion, p. 13.
31. Sato, J. and Tsuji, H. (1983). *Comb. Sci. and Tech.* **33**, p. 193
32. Darabiha, N., Candel, S. and Marble, F. E. (1985). *Comb. and Flame* **64**, p. 203.

RECEIVED June 15, 1987